Magnetic field induced confinement–deconfinement transition in graphene quantum dots



2009 J. Phys.: Condens. Matter 21 102201

(http://iopscience.iop.org/0953-8984/21/10/102201)

IOP FTC

IOP Publishing | Journal of Physics: Condensed Matter

J. Phys.: Condens. Matter **21** (2009) 102201 (6pp) | doi:10.1088/0953-8984/21/10/102201

FAST TRACK COMMUNICATION

# Magnetic field induced confinement–deconfinement transition in graphene quantum dots

**G Giavaras**[1], **P A Maksym and M Roy**

Department of Physics and Astronomy, University of Leicester, Leicester LE1 7RH, UK

Received 25 November 2008
Published 20 January 2009
Online at stacks.iop.org/JPhysCM/21/102201

**Abstract**

Massless Dirac particles cannot be confined by an electrostatic potential. This is a problem for making graphene quantum dots but confinement can be achieved with a magnetic field and here general conditions for confined and deconfined states are derived. There is a class of potentials for which the character of the state can be controlled at will. Then a confinement–deconfinement transition occurs which allows the Klein paradox to be probed experimentally in graphene dots. A dot design suitable for this experiment is presented.

## 1. Introduction

Single layer graphene is attracting attention because its charge carriers are massless, relativistic particles [1]. The relativistic effects result from a unique, zero-gap band structure that leads to quantum states described by the two-component Dirac–Weyl equation. This allows relativistic physics to be explored in a solid state system and has many potential applications ranging from high frequency electronics [1] to quantum computing [2]. In particular, graphene quantum dots are very attractive as spin qubits because they are expected to have low spin decoherence [2]. However there is a problem with making graphene dots for quantum computing or any other application: relativistic effects prevent massless particles from being confined by an external scalar potential.

This problem results from the Klein paradox [3–6]. When relativistic particles with mass are incident on a 1D potential barrier, the state in the barrier decays exponentially unless the barrier height exceeds the threshold for pair production, at which point the state in the barrier becomes oscillatory. The paradox is that any attempt to enhance the localization by increasing the barrier height eventually destroys it. But there is no threshold for pair production for massless particles so exponential decay and bound states do not occur when graphene is subjected to an external potential.

[1] Present address: Department of Materials, Oxford University, Oxford OX1 3PH, UK.

Graphene dots can be formed from external potentials or nanocrystals but this work is only concerned with external potentials. The physics of nanocrystals has been discussed recently [7, 8] and is different from the situation treated here. The quantum states [9–12], in external potentials are quasi-bound: they have a low amplitude oscillatory tail and are similar to the scattering resonances studied in undergraduate physics. A perpendicular magnetic field enhances the localization of these states [10] and true bound states can occur in graphene dots defined by a spatially non-uniform field [11]. So a magnetic vector potential has a localizing effect that tends to cancel the delocalizing effect of a scalar potential. But what are the general conditions for confined states to occur when an electrostatic scalar potential and a magnetic vector potential are applied to graphene simultaneously?

The aim of the present work is to answer this question precisely. It is shown that both true bound states and quasi-bound states occur, depending on the form of the potentials. In addition, there is a third and most interesting possibility. In some cases, the character of the states depends on the parameters of the potentials and can be controlled at will. A confinement–deconfinement transition then occurs in which the character of the states changes from oscillatory to exponential as in the Klein paradox for particles with mass. This gives a way of probing the Klein paradox experimentally in a solid state system and numerical studies of the quantum states in a realistic dot model show it is feasible. Further, the same effect could be used to fabricate a graphene dot

 

which has true bound states. This only requires a uniform magnetic field and a gate which can be made lithographically, a geometry which is much easier to fabricate than the non-uniform magnetic field geometry proposed in [11].

To get more insight into the unique physics of massless, charged particles, consider the one-dimensional barrier in more detail. This is treated in a similar way to a potential barrier for Dirac particles with mass [6] but the lack of mass changes the physics dramatically. Suppose the particles are constrained to move along the $x$-axis and are incident from the left on a potential barrier at the origin. The potential, $V = 0$ when $x < 0$ and $V = U_0$ when $x > 0$ and the particle energy $E$, is positive with $E < U_0$. The graphene particles are described by a two-component wavefunction which satisfies

$$\left(V + \frac{\gamma}{\hbar}\boldsymbol{\sigma}\cdot\mathbf{p}\right)\psi = E\psi, \tag{1}$$

where $\boldsymbol{\sigma}$ are the Pauli matrices, $\mathbf{p}$ is the momentum and $\gamma = 646$ meV nm [10]. The two-component plane waves propagating to the right in the direction normal to the barrier are

$$\begin{aligned} \psi &= \begin{pmatrix} 1 \\ 1 \end{pmatrix} \mathrm{e}^{\mathrm{i}kx}, \qquad x < 0, \\ \psi &= \begin{pmatrix} 1 \\ 1 \end{pmatrix} \mathrm{e}^{\mathrm{i}k'x}, \qquad x > 0, \end{aligned} \tag{2}$$

where $\hbar^2k^2 = E^2/c^2$, $\hbar^2k'^2 = (E - U_0)^2/c^2$ and the particle speed is $c = \gamma/\hbar$. The boundary condition at the origin is that both components of the wavefunction are continuous [6]. This is clearly satisfied without any reflected waves so the transmission coefficient is 100% and the barrier does not constrain the motion of the particles.

The fact that the transmission is 100% regardless of $E$ and $U_0$ is a consequence of the zero mass. If the particles had mass $m_0$, the energy–momentum relation would be $(E - V)^2 - p^2c^2 = m_0^2c^4$ and the amplitudes of the wavefunction components in equations (2) would depend on $k$ or $k'$ and $m_0$ [6]. Then the right side amplitude in equations (2) would be different from the left side amplitude so a reflected wave would have to be introduced to satisfy the boundary condition at $x = 0$ and the transmission coefficient would not be 100%.

Remarkably, classical massless, charged particles can also penetrate the barrier. When these particles are incident on the barrier, their momentum changes so that $(E - V)^2 = p^2c^2$ is always satisfied, however the speed $c$ remains constant. The resulting trajectories depend on the boundary condition at $x = 0$. If the position and velocity are chosen to be continuous, particles incident from the left penetrate the barrier and carry on moving to the right with constant speed $c$. So the transmission coefficient is 100% as in quantum mechanics. The lesson to be learnt from this is that the physics of charged particles which have to keep moving is completely different from the physics of those that are able to stop.

The effects in two dimensions are even more dramatic because the velocity vector can change direction continuously and can be influenced by a magnetic field. This is investigated here with the aid of a graphene dot model. The system is cylindrically symmetric and the dot region is defined by an electrostatic potential, $V(r)$. The magnetic field is perpendicular to the plane of the dot and the magnetic vector potential, $A_\theta(r)$, is in the azimuthal ($\theta$) direction. When the system is treated with quantum mechanics it is found that the functional form of the potentials has a dramatic effect on the character of the states. In particular, when $V$ and $A_\theta$ increase as power laws, $V = V_0r^s$, $A_\theta = A_0r^t$, $s, t > 0$, the character of the states depends critically on $s$ and $t$. If $s > t$ the states oscillate in the asymptotic regime of large $r$ but decay exponentially when $s < t$. In both cases the asymptotic character of the states is independent of $V_0$ and $A_0$ but when $s = t$ the character of the states does depend on these constants and a transition from exponential to oscillatory behaviour occurs when $V_0$ is increased or $A_0$ is decreased. This is the confinement–deconfinement transition which may be the key to fabricating a graphene quantum dot.

## 2. Theory of confinement–deconfinement transition

The two-component envelope function, $\psi$, satisfies equation (1) with the momentum $\mathbf{p}$ replaced by $\boldsymbol{\pi} = \mathbf{p} + e\mathbf{A}$. For cylindrically symmetric systems the two-component state is

$$\psi = \begin{pmatrix} \chi_1(r)\exp(\mathrm{i}(m-1)\theta) \\ \chi_2(r)\exp(\mathrm{i}m\theta) \end{pmatrix},$$

where $m$ is the angular momentum quantum number and the radial functions $\chi_1$ and $\chi_2$ satisfy

$$\frac{V}{\gamma}\chi_1 - \mathrm{i}\frac{\mathrm{d}\chi_2}{\mathrm{d}r} - \mathrm{i}\frac{m}{r}\chi_2 - \mathrm{i}\frac{e}{\hbar}A_\theta\chi_2 = \frac{E}{\gamma}\chi_1, \tag{3}$$

$$-\mathrm{i}\frac{\mathrm{d}\chi_1}{\mathrm{d}r} + \mathrm{i}\frac{(m-1)}{r}\chi_1 + \mathrm{i}\frac{e}{\hbar}A_\theta\chi_1 + \frac{V}{\gamma}\chi_2 = \frac{E}{\gamma}\chi_2. \tag{4}$$

To analyse the character of the states, a single equation for $\chi_2$ or $\chi_1$ is needed. This is found by differentiating equations (3) and (4) which leads to the relation

$$\chi_2'' + a(r)\chi_2' + b(r)\chi_2 = 0, \tag{5}$$

where

$$a(r) = \frac{1}{r} + \frac{1}{E - V}\frac{\mathrm{d}V}{\mathrm{d}r}, \tag{6}$$

$$b(r) = -\frac{m^2}{r^2} + \left(\frac{m}{r} + \frac{e}{\hbar}A_\theta\right)\frac{1}{E - V}\frac{\mathrm{d}V}{\mathrm{d}r} - \frac{(2m-1)}{r}\frac{e}{\hbar}A_\theta + \frac{e}{\hbar}\frac{\mathrm{d}A_\theta}{\mathrm{d}r} + \frac{(E - V)^2}{\gamma^2} - \frac{e^2}{\hbar^2}A_\theta^2. \tag{7}$$

The first order derivative in equation (5) is eliminated by putting $\chi_2(r) = u_2(r)\exp(-\int a(r)\,\mathrm{d}r/2)$ which gives

$$u_2'' + k_2^2(r)u_2 = 0, \tag{8}$$

where $k_2^2(r) = b - a'/2 - a^2/4$. Although $k_2^2$ diverges when $E = V$, $\chi_2$ is regular there. Since $\exp(-\int a(r)\,\mathrm{d}r/2)$ is not an oscillatory function of $r$, $u_2$ has the same character as $\chi_2$. Equation (8) shows that this character is oscillatory when $k_2^2$ is positive and exponential when $k_2^2$ is negative. Asymptotic exponential decay is characteristic of a bound state but here

'confined' is used to indicate a bound state that is localized near the centre of the dot.

When $V$ and $A_\theta$ increase as power laws, the asymptotic form of $k_2^2$ is $(V_0/\gamma)^2 r^{2s} - (eA_0/\hbar)^2 r^{2t}$. Hence $k_2^2$ is positive when $s > t$, leading to oscillatory character and deconfined states. And $k_2^2$ is negative when $s < t$, leading to exponential character and confined states. However if $s = t$ the asymptotic form is $[(V_0/\gamma)^2 - (eA_0/\hbar)^2]r^{2t}$ so the sign of $k_2^2$ depends on $V_0$ and $A_0$ and a confinement–deconfinement transition occurs when $V_0^2 = (\gamma e A_0/\hbar)^2$. This also follows from the uncoupled equation for $\chi_1$: the corresponding $k^2$-value, $k_1^2 \neq k_2^2$ but $k_1^2 \to k_2^2$ in the asymptotic limit so $\chi_1$ and $\chi_2$ have the same character.

Just like the 100% transmission of a one-dimensional barrier, the quantum confinement–deconfinement transition for a two-dimensional dot has an exact classical analogue and this takes the form of a change in the character of classical orbits around the centre of the confining potential. In two dimensions, the classical energy–momentum relation is $c^2 p_r^2 = (E - V)^2 - c^2(M/r + eA_\theta)^2$, where $M$ is the angular momentum, $r$ is the radial co-ordinate and $p_r$ is the radial component of the momentum. $p_r^2$ is shown in figure 1 for a system that undergoes a confinement–deconfinement transition. The classically allowed region is where $p_r^2 \geqslant 0$ and is delimited by the roots of $p_r^2 = 0$. On the low field side of the transition ($B = 0$ and 0.6 T), there are three roots. Bounded classical motion occurs between the first two (between 14 and 96 nm at $B = 0$ T) and this is analogous to elliptic orbits in the classical Kepler problem. In addition, unbounded motion is allowed when $r$ exceeds the third root (beyond 121 nm at $B = 0$ T) and this is similar to parabolic and hyperbolic orbits in the classical Kepler problem. But, unlike the Kepler case, both bounded and unbounded motion are allowed at the same energy. The unbounded motion corresponds to deconfined quantum states. However, the third root disappears on the high field side of the transition ($B = 1.2$ T) and only bounded motion occurs, corresponding to confined states. So there is a change in the allowed classical motion that corresponds to the quantum confinement–deconfinement transition. The correspondence is exact because the disappearance of the third root is connected with a change in the asymptotic sign of $p_r^2$ and in the asymptotic regime $p_r^2$ differs from $k^2$ only by a factor of $\hbar^2$, leading to identical conditions for the classical and quantum transitions.

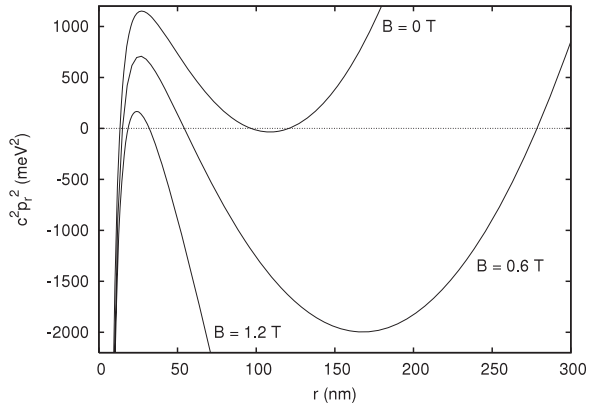


**Figure 1.** Classical radial momentum for a system that undergoes a confinement–deconfinement transition. The system parameters are, $s = 1$, corresponding to a linear potential with $V_0 = 0.5$ meV nm$^{-1}$ and $t = 1$, corresponding to a uniform magnetic field as indicated in the figure. The particle energy is 55 meV and the angular momentum is $\hbar$.

## 3. Numerical studies of model states

To investigate the unusual quantum states of a graphene dot further, equations (3) and (4) are solved numerically and the objective of these studies is to distinguish confined states from deconfined states. The Hamiltonian, $H$, satisfies

$$\int_0^R \int_0^{2\pi} \left[\psi_\alpha^* H \psi_\beta - (H\psi_\alpha)^* \psi_\beta\right] \mathrm{d}\theta r \, \mathrm{d}r = -2\pi \mathrm{i}\gamma \left[(\chi_{1\alpha}^* \chi_{2\beta} + \chi_{2\alpha}^* \chi_{1\beta}) r\right]_0^R, \quad (9)$$

where $\psi_\alpha$ and $\psi_\beta$ are two-component states of angular momentum $m$ and $\chi_{i\alpha}$ and $\chi_{i\beta}$ are the corresponding radial functions. Equations (3) and (4) lead to a Hermitian eigenvalue problem when the boundary terms in equation (9) vanish. For this to happen it is sufficient that one component is regular at the origin and one component vanishes at the boundary, $R$. Then it follows from equations (3) and (4) that both components are regular at the origin but it does not follow that both components vanish at $R$. However a true bound state has an exponential tail so both components of a bound state vanish in the limit of large $R$. Hence confined and deconfined states can be distinguished by solving equations (3) and (4) subject to the boundary conditions that one component is regular at the origin and *one* component vanishes at $R$ and then looking for an exponential tail in *both* components.

Equations (3) and (4) are solved by discretizing them on a uniform grid. By applying the time reversal operator to equations (3) and (4) it can be shown that $E(m, A_0) = E(1 - m, -A_0)$. It is important to ensure that the eigenvalues of the discretized Hamiltonian have the same property and this requires identical numbers of grid points for $\chi_1$ and $\chi_2$. This excludes the use of centred differences so $\mathrm{d}/\mathrm{d}r$ is approximated by the forward difference operator $L_\mathrm{f}$ or the backward difference operator $L_\mathrm{b}$. The procedure depends on $m$. When $m \leqslant 0$, $\chi_2(R)$ is chosen to vanish, $L_\mathrm{f}$ is used to find $\mathrm{d}\chi_2/\mathrm{d}r$ and $L_\mathrm{b}$ to find $\mathrm{d}\chi_1/\mathrm{d}r$ and vice versa when $m \geqslant 1$. Although this guarantees that $E(m, A_0) = E(1 - m, -A_0)$, it has the disadvantage that numerical errors are linear in the step length $\Delta r$. To compensate for this, $\Delta r$ is kept small and all the eigenvalues computed in this work are accurate to about 1 part in $10^3$, except for $s = 2, t = 1$ and $s = 2, t = 2$, where there are rapid oscillations but the accuracy is still better than 2%. The discretization leads to a non-Hermitian matrix eigenvalue problem. A similarity transformation is used to reduce this to a real, symmetric eigenvalue problem which is solved numerically.

For brevity, all the quantum states shown in the present work are $m = 1$ states. It has been verified that other states exhibit similar features, although the amplitude of oscillations is $m$-dependent [10]. Since the main focus of this work is on the confinement–deconfinement transition, the

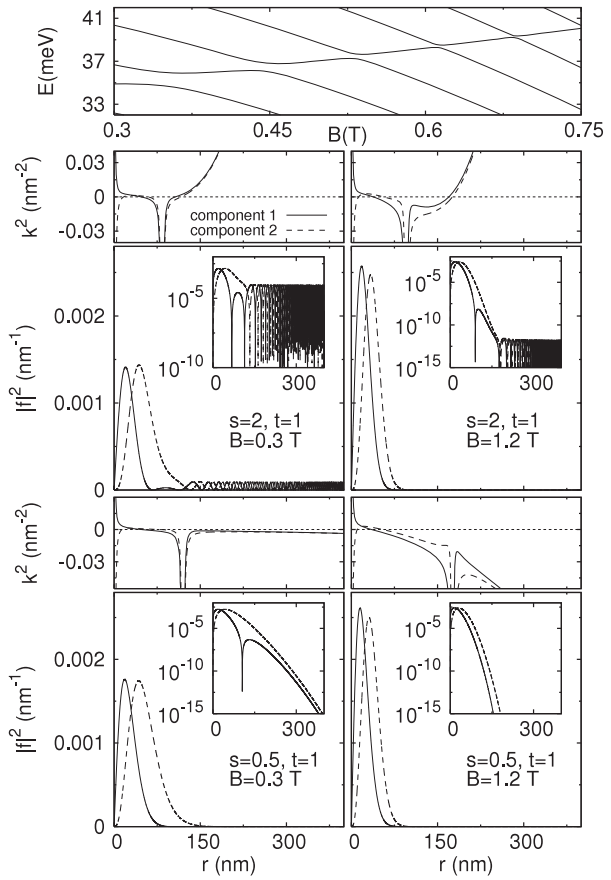


**Figure 2.** Confined and deconfined states for cases when no transition occurs. The frame above each state shows $k_i^2$. Topmost frame: $E(B)$ for $s = 2, t = 1$.

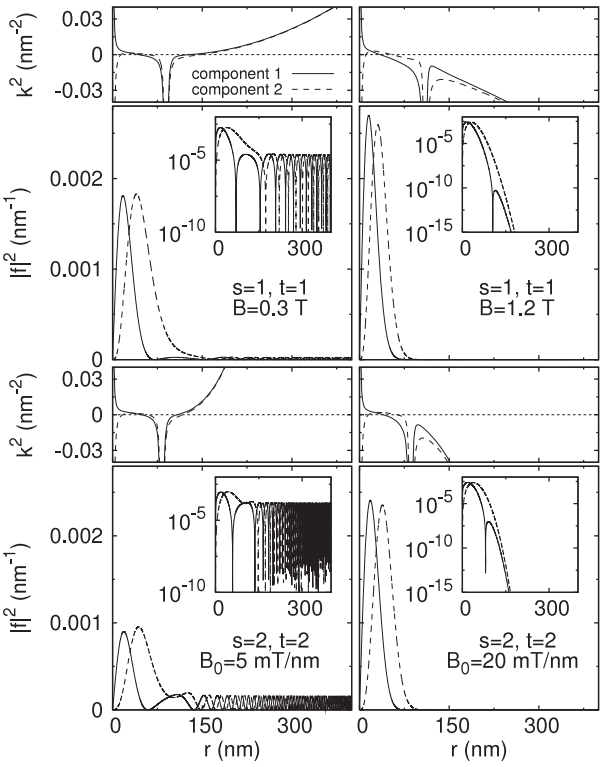


**Figure 3.** As figure 2 but for two cases which exhibit a confinement–deconfinement transition.

states are selected so that the behaviour at the origin does not change significantly when the potential parameters are changed. All the states have been selected to have a large amplitude close to the origin and can be regarded as dot states. The energies as a function of magnetic field typically show a series of anti-crossings (figure 2) but in many cases the anti-crossings disappear at a sufficiently high magnetic field. Where necessary, the line of anti-crossings is followed to preserve the qualitative form of the state at the origin. Every energy computed here is between 26 and 67 meV, within the validity limit of the linear graphene Hamiltonian ($\approx \pm 1$ eV [1]).

Confined and deconfined states are illustrated in figure 2. The radial probability distribution, $|f_i|^2 \equiv r|\chi_i|^2$, $i = 1, 2$ is shown together with $k_i^2$. The insets show $|f_i|^2$ on a logarithmic scale. $R = 600$ nm, large enough to ensure that the asymptotic sign of $k_i^2$ has been reached. The magnetic field, $B$, is uniform. When $s = 2$, $t = 1$, $V_0 = 5 \times 10^{-3}$ meV nm$^{-2}$, the asymptotic sign of $k_i^2$ is positive and the asymptotic character of $|f_i|^2$ is oscillatory, independent of $B$. The amplitude of the oscillations decreases with increasing $B$. When $s = 0.5, t = 1$, $V_0 = 5$ meV nm$^{-1/2}$ and $B \neq 0$, the asymptotic sign of $k_i^2$ is negative and the asymptotic character of $|f_i|^2$ is exponential, as can be seen from the insets.

The confinement–deconfinement transition is illustrated in figure 3. $R = 600$ nm, again large enough to reach the asymptotic regime. When $s = 1$, $t = 1$, $V_0 = 0.5$ meV nm$^{-1}$ and $B = 0.3$ T, the asymptotic sign of $k_i^2$ is positive and the asymptotic character is oscillatory. In contrast, when $B = 1.2$ T, the asymptotic sign of $k_i^2$ is negative and the asymptotic character is exponential. The transition also occurs in non-uniform magnetic fields and it may be possible to generate a suitable field by putting a dot under a superconducting obstacle in a uniform field. Figure 3 (bottom) shows the transition for $s = 2$, $t = 2$, $V_0 = 5 \times 10^{-3}$ meV nm$^{-2}$, that is parabolic confinement in a linearly increasing field, $B(r) = B_0 r$.

## 4. Numerical studies of realistic states

In any real quantum dot, the scalar potential would approach a finite asymptotic value instead of increasing without limit. Consequently, all the states of a graphene dot in a magnetic field have an exponential tail. However, an effect similar to the confinement–deconfinement transition occurs in the middle distance region between the centre of the dot and the asymptotic regime.

For this transition to be observable, the dot level has to be in the region of very low density of states between the bulk Landau levels. This requires a potential similar to the one shown in figure 4. The asymptotic value of the potential is engineered to be just below the dot level. This puts the dot level between the zeroth and first Landau levels. Thus the dot level can be isolated from the bulk Landau levels provided that they are narrow enough.

The required potential can be generated by gate electrodes. One possible arrangement is a metal plate with a circular

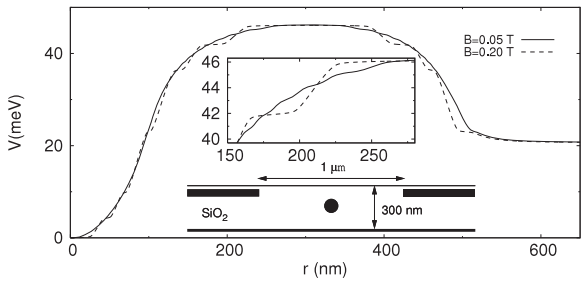


**Figure 4.** $V(r)$ for the gate geometry shown in the bottom inset.

hole that contains an electrode. The graphene sheet is above these electrodes on 300 nm of $SiO_2$ on a back-gate at 0 V. The plate ($-1$ V) generates the asymptotically flat part of the potential, the hole generates the barrier and the central electrode ($-2$ V) generates the well. Similar gated, monolayer graphene nanostructures have been fabricated recently [13]. The potential in figure 4 was computed by solving the Poisson equation on a discrete mesh. Screening by the graphene sheet was treated in the Thomas–Fermi approximation [14]. The resulting potential is magnetic field dependent because the density of states is field dependent. This causes steps in the potential (inset to figure 4) which occur when the number of occupied Landau levels changes. However the field dependence is weak at the low fields considered here.

The confinement–deconfinement transition effect for the potential in figure 4 and a uniform magnetic field is shown in figure 5. For all fields, the states have a peak near the centre of the dot and an exponential tail. The transition occurs in the middle distance region between these two features, between about 200 and 400 nm. For any potential, the middle distance region can be identified by computing $k_i^2$. In figure 5, this varies rapidly because of the steps in the potential but remains positive in the middle distance region when $B = 0.05$ T. At this field, the oscillations in $|f_i|^2$ correspond to those in figure 3 but are much less rapid because $V$, hence $k_i^2$ is smaller. As the field increases the region of positive $k_i^2$ shrinks and a transition to exponential behaviour occurs. This is analogous to the change of character seen in the Klein paradox for relativistic particles with mass.

The occurrence of the transition is insensitive to the electrode geometry. The one in figure 4 has the advantage that the graphene is easy to access but may be difficult to fabricate. However, similar transitions occur in systems with disk or spherical central electrodes with the plate and central electrode either above or below the graphene sheet. In addition, calculations for model potentials with a well, barrier and flat portion show that the occurrence of the transition is insensitive to the model parameters. The only requirement is a region where $k_i^2$ changes sign when $A_0$ increases. This is relatively easy to arrange.

$|f_i|^2$ in figure 5 decreases by 3–4 orders of magnitude at $r \approx 300$ nm when the character of the state changes from oscillatory to exponential. This large effect could be used to probe the transition experimentally. For example, the decrease in $|f_i|^2$ causes a decrease in the local density of states (LDOS) near the dot which could be detected with scanning tunnelling

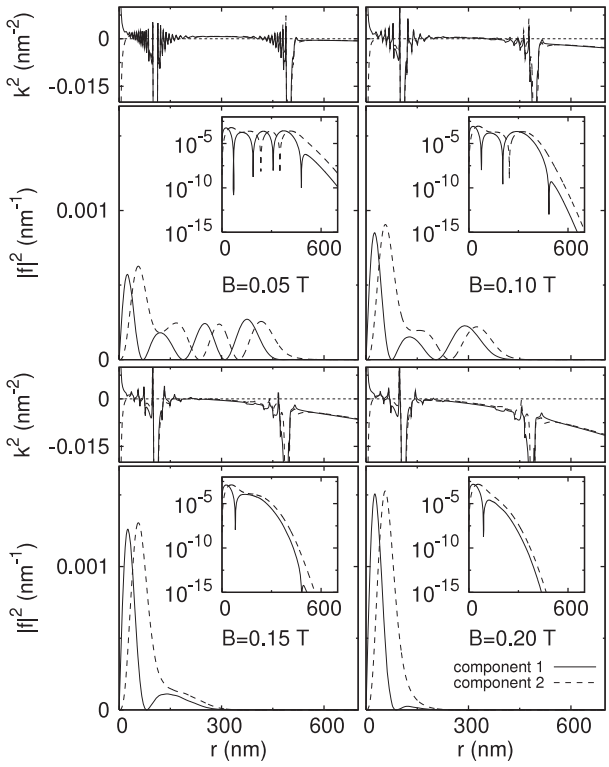


**Figure 5.** Confinement–deconfinement transition. As figure 3 but for the potential shown in figure 4.

microscopy. The decrease in $|f_i|^2$ would also cause a large decrease in the overlap of the dot state with states in contacts at $r \approx 300$ nm. This could be detected by looking for a change in transport through the dot state via diametrically opposite contacts at $r \approx 300$ nm. Numerical calculations of the LDOS for the potential in figure 4 show that the state in figure 5 lies in a region of very low bulk density of states, with the dot state around 0.1–0.2 meV away from any other levels. This suggests the dot state can be resolved experimentally in graphene samples of sufficient quality.

## 5. Conclusion

Confined and deconfined states occur in graphene dots in a magnetic field. When the vector and scalar potentials increase with a power law, the states are confined when the scalar potential rises slowly compared to the vector potential and deconfined when it rises rapidly. But when the scalar and vector potentials have the same power law, a confinement–deconfinement transition occurs. This effect corresponds exactly to a change in the character of the classical motion and confined quantum states occur only when unbounded classical motion is forbidden. When the transition occurs, the character of the quantum states can be controlled at will by adjusting the dot parameters and the magnetic field. A similar effect occurs in a realistic dot model. This is analogous to the relativistic Klein paradox and could be observed experimentally via transport studies or STM. Experiments of this kind would give insight into the unusual physics of classical massless charged

particles as well as the unique quantum states of a graphene dot. The proposed system may be attractive because it allows graphene dots to be formed with well-established lithographic techniques and only requires a uniform magnetic field.

## Acknowledgments

It is a pleasure to acknowledge useful discussions with Professors H Aoki, H Fukuyama and S Tarucha. We thank Professor J L Beeby for some very helpful comments on our manuscript. This work was supported by the UK Engineering and Physical Sciences Research Council.

## References

[1] Geim A K and Novoselov K S 2007 *Nat. Mater.* **6** 183
[2] Trauzettel B, Bulaev D V, Loss D and Burkard G 2007 *Nat. Phys.* **3** 192
[3] Katsnelson M I, Novoselov K S and Geim A K 2006 *Nat. Phys.* **2** 620
[4] Peres N M R, Castro Neto A H and Guinea F 2006 *Phys. Rev.* B **73** 241403(R)
[5] Cheianov Vadim V and Fal'ko Vladimir I 2006 *Phys. Rev.* B **74** 041403(R)
[6] Bjorken J D and Drell S D 1964 *Relativistic Quantum Mechanics* (New York: McGraw-Hill) chapter 3
[7] Schnez A, Ensslin K, Sigrist M and Ihn T 2008 arXiv:0810.3216v1
[8] Peres N M R, Rodriquez J N B, Stauber T and Lopes dos Santos J M B 2008 arXiv:0810.4768v1
[9] Silvestrov P G and Efetov K B 2007 *Phys. Rev. Lett.* **98** 016802
[10] Chen H-Y, Apalkov V and Chakraborty T 2007 *Phys. Rev. Lett.* **98** 186803
[11] De Martino A, Dell'Anna L and Egger R 2007 *Phys. Rev. Lett.* **98** 066802
[12] Matulis A and Peeters F M 2008 *Phys. Rev.* B **77** 115423
[13] Huard B, Sulpizio J A, Stander N, Todd K, Yang B and Goldhaber-Gordon D 2007 *Phys. Rev. Lett.* **98** 236803
[14] DiVincenzo D P and Mele E J 1984 *Phys. Rev.* B **29** 1685